NATIONAL AERONAUTICS AND SPACE ADMINISTRATION

EARTH RESOURCES SURVEY PROGRAM

INTERAGENCY REPORT NASA-91

FAR INFRARED LUMINESCENCE

By

A. E. Stoddard
U.S. Geological Survey
Washington, D.C.

October 1967

Prepared by the Geological Survey for the
National Aeronautics and Space Administration (NASA)
under NASA Contract No. R-146-09-020-006 and T-65754

MANNED SPACECRAFT CENTER
HOUSTON, TEXAS

UNITED STATES
DEPARTMENT OF THE INTERIOR
GEOLOGICAL SURVEY
WASHINGTON, D.C. 20242

Interagency Report
NASA-91
October 1967

Dr. Peter C. Badgley
Program Chief,
Earth Resources Survey
Code SAR - NASA Headquarters
Washington, D.C. 20546

Dear Peter:

Transmitted herewith is one copy of:

INTERAGENCY REPORT NASA-91

FAR INFRARED LUMINESCENCE*

by

A. E. Stoddard**

The U.S. Geological Survey has released this report in open files. Copies are available for consultation in the Geological Survey Libraries, 1033 GSA Building, Washington, D.C. 20242; Building 25, Federal Center, Denver, Colorado 80225; 345 Middlefield Road, Menlo Park, California 94025; and 601 E. Cedar Avenue, Flagstaff, Arizona 86001.

Sincerely yours,

William A. Fischer
Research Coordinator
Earth Orbiter Program

*Work performed under NASA Contract No. R-146-09-020- 006 and T-65754
**U.S. Geological Survey, Washington, D.C.

UNITED STATES
DEPARTMENT OF THE INTERIOR
GEOLOGICAL SURVEY

INTERAGENCY REPORT: NASA-91

FAR INFRARED LUMINESCENCE*

by

A. E. Stoddard**

October 1967

Prepared by the U.S. Geological Survey
for the National Aeronautics and Space
Administration (NASA)

*Work performed under NASA Contract No. R-146-09-020-006 and T-65754

**U.S. Geological Survey, Washington, D.C.

CONTENTS

Page

Abstract 1

Introduction 2

Apparatus 4

Calibration 7

Results 9

Discussion 11

FIGURES

Figure 1 - A schematic, cut-away drawing of the detector apparatus 15

Figure 2 - A schematic, cut-away drawing of the sample mounting 16

Figure 3 - Curves showing typical results of the recorder detector signal with no filter (A) and at different wavelengths (B), (C), (D) 17

Figure 4 - Curves showing rise in detector signal in response to radiation at different wavelengths when $T = -180^{o}C$ 18

Figure 5 - Curves showing rise in detector signal in response to radiation at different wavelengths when $T = 0^{o}C$ 19

Figure 6 - Average curves (lines) showing best fit relation to points derived from mathematical model 20

Figure 7 - Curves showing rise in detector signal when luminescent radiation within the filter pass band is superimposed on the thermal radiation from the sample, where (A) $T = -180^{o}C$ and (B) $T = 0^{o}C$ . . . 21

FAR INFRARED LUMINESCENCE

by

A. E. Stoddard

ABSTRACT

The rise in intensity of 8.6 - 20μ infrared radiation from surfaces of quartz monzonite, dunite and tektite illuminated by visible light has been studied for a range of initial surface temperatures from -180°C to 0°C. No departures in the rise curves from the predicted increase in thermal radiation with illumination time were observed. Upper limits to the efficiency of a luminescent process in these materials which would introduce a prompt rise in infrared emission at the onset of illumination are found to be 0.02% at surface temperatures of -180°C and 0.25% at 0°C.

FAR INFRARED LUMINESCENCE

by

A. E. Stoddard

INTRODUCTION

Emission of infrared radiation from solids is generally studied in one of two ways: First, the sample, in the form of a slab, is heated from one side to a desired temperature and infrared emission from the other side is collected in a spectrometer which measures the radiation spectrum. Second, the sample is irradiated by a black body and the reflected radiation is collected and analyzed. Kirchoff's law, relating emissivity to the measured reflectivity, applies in this case if the black body and sample surface temperatures are the same. Emission from the sample is given by the calculated emissivity and the Planck distribution function. These two methods yield the same results when properly applied.

Neither of these methods, however, measures infrared emission from a solid under the common circumstance that the solid is illuminated by light from the sun on the same surface from which emission is observed. The emission is generally assumed, in this case, to be that measured by these methods from a sample at the temperature of the illuminated surface. The purpose of this research is to make a preliminary investigation of whether or not this assumption is valid. Is there luminescence in the far infrared when a solid is illuminated by visible light?

The excitation of a solid produced in either method of measuring infrared emission, for temperatures corresponding to terrestrial or lunar conditions, consists almost entirely of lattice vibrational energy. When a solid is illuminated by visible light, on the other hand, the solid is raised to excited electronic states. To the extent that these states are de-excited by their coupling to the lattice some of the excitation energy diffuses among the lattice vibrations, resulting in the emission of infrared radiation. Were the illumination stopped, then the lattice energy would assume the equilibrium frequency spectrum corresponding to the sample temperature. During illumination, however, the frequency spectrum at the illuminated surface is conceivably quite different, resulting in anomalous infrared emission, or luminescence.

Luminescent infrared emission from an illuminated solid would depend upon the mechanism of coupling between excited electronic states and lattice vibrations, and upon the strength with which lattice vibrations are coupled to one another to bring about their equilibrium frequency spectrum. As an hypothesis, the electronic states are presumed to be strongly coupled to those lattice vibrations whose frequencies are the "characteristic frequencies" of the lattice, and only weakly to others. The energy input to the lattice would then be peaked about lattice vibrations of these frequencies. If coupling of lattice vibrations to one another is not too strong the resulting vibrational spectrum during illumination will retain peaks about the characteristic frequencies, with these peaks also in the spectrum of emitted infrared.

Evidence is sought for this hypothesis in the rate of increase of infrared emission, in the wavelength region of the lattice characteristic frequencies, at the beginning of visible illumination. The vibrational spectrum peak would be established concurrently with the excitation of electronic states, so that luminescent, infrared radiation generated by these lattice vibrations would rise in intensity at the same rate as the reflected visible radiation. Thermal infrared radiation rises more slowly in response to the increase in temperature of the sample. Direct spectral analysis of the emitted infrared, particularly at the low temperatures employed, is beyond the present facilities of this experiment.

APPARATUS

A schematic, cut-away drawing of the apparatus is shown in figure 1. Part of a two liter liquid nitrogen resevoir is shown at the top, within an outer vacuum shell enclosing the entire apparatus. The experiment is designed for a range of temperatures, with a low of approximately -180°C, for several reasons. The low temperature allows reproduction of lunar as well as terrestrial temperature conditions. Also, since the ambient thermal radiation from a solid drops rapidly with temperature, the background above which luminescence is to be observed is greatly reduced at the lower temperature. Additionally, a wide temperature range is desirable since the de-excitation of the solid after absorption of visible radiation likely depends upon the degree of lattice excitation. The mechanism of luminescence may thus be temperature dependent.

The sample, figure 1, is enclosed by materials at liquid nitrogen temperature. Most of this enclosure consists of aluminum coated with Parson's Black to be almost totally absorbing. The optical path indicated by the horizontal dashed line through the vacuum shell is closed to infrared radiation by a one centimeter long cylinder of fused quartz which is cooled within a housing attached to the main aluminum block. The quartz is nearly opaque to radiation of wavelength greater than 4 microns and, due to its low temperature, radiates little infrared. The path for a second external source is located at 90° from the one shown, in the cut-away region. This path is generally closed by a cooled beryllium window and is then used for x-ray irradiation of the sample.

Greater detail of the sample mounting is shown in figure 2. The sample is spring clipped to a copper plate for temperature uniformity. This plate is backed by a stainless steel one with a recess for a thermocouple and a 100 ohm heating coil. This assembly is supported by three teflon covered rods from a back plate attached to the main aluminum cold block. A metal bellows joins the recessed plate and the back plate, and is connected by metal capillary tubing to the outside of the vacuum shell. When the bellows are evacuated through the tubing, the sample holder assembly is spring loaded back against the teflon supports to isolate the sample from the cold aluminum block. When the tubing is externally switched to connect to helium at 20 psi gauge pressure, the bellows extend to force the copper sample plate against the aluminum. The sample may thus be cooled to liquid nitrogen temperature with the bellows pressurized, or warmed by the heater when isolated by evacuation of the bellows.

Radiation from the sample is reflected downward through a filter wheel by a gold plated mirror, as shown in figure 1. The filter wheel provides limited spectral information for radiation from the source. It is fitted with three cooled infrared filters, for the bands 3.2 and 6.6 microns, 8.6 to 10.7 microns and 10.6 to 20 microns respectively, and a blank for total radiation. The wheel is rotated from outside the vacuum shell from below as indicated, with a teflon shaft coupling.

Radiation passing the filter wheel is collected in a polished cone and delivered to a cooled, Epply wire-wound thermopile.

Operation of the complete assembly is indicated by the dashed line in figure 1. An external source of radiation is directed upon the sample within the cooled enclosure. Radiation from the sample generated by this external source is reflected through a filter wheel for spectral analysis and detected by the thermopile. External circuitry consists of an operational amplifier and an X-T recorder to present the detector signal, a DC power supply for the sample heater and a millivolt recorder to measure the thermocouple emf.

The primary source of external radiation used to date is an Edmund "Tru-Focus," 150 watt projection lamp. The AC power for this lamp is controlled by a darkroom timer which has been modified to provide an output signal when switched on or off, to mark the period of illumination on the detector signal recorder. An x-ray source has been used on a few occasions.

CALIBRATION

Approximate values for the sensitivity of the detector for radiation from the sample, and for the intensity of external radiation incident upon the sample are necessary for semiquantitative results.

The design estimate of the detector sensitivity was made from the manufacturers suggested value of 0.1 volt per watt per cm^2 of radiation incident upon the detector. This value may be expressed in terms of radiation from the source rather than radiation incident upon the detector. The collecting cone over the detector effectively enlarges its size to that of the illuminated portion of the sample. The angle factor for this sample-detector configuration, that is, the fraction of radiation emitted by the sample which reaches the detector, is calculated to be 2.5%. For design purposes, then, the detector sensitivity was estimated to be 2.5×10^{-3} volt per watt per cm^2 of energy radiated by the sample within the pass band of the filter between sample and detector.

The measured detector sensitivity exceeds this estimate by almost an order of magnitude. The actual sensitivity was determined by measuring the rise in detector signal with a known increase in sample temperature. The signal was nulled with the sample at low temperature and measured after the sample and holder had reached equilibrium at a higher temperature. A signal of 40μvis observed, for example, with an increase of sample temperature from -181°C to -86°C and with the 10.6 - 20 micron filter in the radiation path. Assuming the sample emissivity to be unity for this calculation and the filter to pass 80% of the radiation within its pass band, then the radiation per unit area

of sample which passes the filter at these two temperatures is 1.4 x 10^{-5} and 2.1 x 10^{-3} watts per cm^2 respectively. The sensitivity is thus 0.019 volts per watt per cm^2. The same value is obtained, as expected, with the filter removed.

The experimental procedure for determining detector sensitivity would be in error were the temperature of the thermopile reference junctions to rise during the prolonged period during which the sample is at elevated temperature. Such an effect would decrease the signal below the correct value. This possibility was ruled out by placing an aluminum disc in the filter position, with a polished face toward the detector. After equilibration, the 10.6 - 20 micron filter was rotated into position and the signal measured immediately. As before, the signal was constant at 40μv.

The intensity of external radiation at the position of the sample was measured with a simple radiation probe. The probe was constructed of a 1/2" square of 21 mil copper sheet, painted with Parson's Black on the front face and with a thermocouple soldered to the rear. It was mounted in the position of the sample, and the dewar evacuated to insulate the probe during illumination. When illuminated, a linear initial rise in temperature of the probe is observed with a theoretical rate FA/MC, where F is the incident intensity and A, M and C are the probe area, mass and specific heat respectively. The measured intensity of the Edmund projection lamp at the sample position is 0.4 watts per cm^2.

RESULTS

Performance of the apparatus was studied by removing the sample to expose the sample support plate to external radiation. The gold surface of this plate has very high reflectivity and low emissivity so that radiation reaching the detector under this condition is a base for comparison with signals observed from mineral samples. Typical results are shown in figure 3, in which traces of the recorder detector signal as a function of time during and after illumination by the Edmund lamp are presented. The plate temperature was -168°C during these runs.

No filter was interposed between the sample and detector in figure 3A. Filters were present in cases B, C and D with the wavelength pass bands indicated. The zero of time is the beginning of illumination and "end" denotes termination of illumination. The scale on the vertical axes is the output voltage of the detector and changes by a factor of 200 from the first to the last two traces.

Traces A and B of figure 3 are interpreted to represent radiation from the lamp which passes the one centimeter quartz input filter and is reflected by the plate to the detector. Some of this radiation lies in the pass band of the 3.2 - 6.6μ filter as expected. The rise and decay of these traces is exponential with a time constant of 0.9 seconds.

Traces C and D of figure 3 show that no detectable increase in radiation of wavelength between 8.6 and 20μ is generated within the interior of the apparatus during illumination. In particular, no discernable rise in temperature of the quartz input filter occurs which would radiate into the interior. These traces also demonstrate that the two infrared filters pass a neglegible fraction of the incident visible light entering the interior through the quartz filter.

Samples were prepared from three widely differing rock types: quartz monzonite, dunite and a tektite supplied by Dr. E.C.T. Chao, U. S. Geological Survey. Each was cut to a slab 1/16" thick and 1" square, with the side fitting against the sample plate polished. The system was typically equilibrated overnight at a low temperature, after which the temperature of the sample mounting plate was approximately -180°C. Each sample was illuminated by the Edmund lamp for various intervals of time at this temperature and the detector response recorded with various filters in the optical path. The sample assembly was then thermally isolated by evacuation of the bellows and raised to various temperatures as high as 0°C. Illumination was repeated at each of these higher temperatures. The results for each sample are very similar, so that only those for the last sample studied, the tektite, are reproduced here.

Figures 4 and 5 show the rise in detector signal in response to radiation from the sample passing the 8.6 - 10.7μ and 10.6 - 20μ filters, for illumination at sample temperatures of -180°C and 0°C, respectively.

The solid curves are particular recorder traces and the dashed curves visual averages of several traces. Illumination began at the zero of each curve and continued approximately 10 seconds. These results are characteristic of those obtained for all three samples for various periods of illumination from 3 to 20 seconds, and for sample temperatures intermediate between -180°C and 0°C.

Attempts were also made to observe infrared radiation from the sample using ultraviolet and x-ray excitation. The intensity of the mercury arc, ultraviolet lamp is approximately 0.06 milliwats per cm^2

at the sample position, compared to the 0.4 watts per cm^2 Edmund lamp intensity. The x-ray beam was generated at a distance of approximately 10" from the sample by a 25 ma current of 50KV electrons. No infrared radiation was observed with excitation from either of these sources.

DISCUSSION

The shape of the curves in figures 4 and 5 suggest that they arise from thermal radiation emitted by the sample as its temperature rises during illumination. No signal increase with the time constant of the detector, as in figures 3A and 3B, are observed.

The thermal behavior of the sample may be readily calculated with certain simplifications. The relatively slow signal decay after illumination corresponds to a heat flux into the copper mounting plate of some 0.05 watts per cm^2 when the sample is at its maximum temperature in figure 4B. This flux is much smaller at the beginning of illumination, and is sufficiently small compared to the incident 0.4 watts per cm^2 that the sample may be approximated as an insulated slab during illumination. The characteristic time for heat flow in such a slab is $\ell^2/\pi^2\kappa$, where ℓ is the slab thickness and κ its diffusivity. The tektite sample is 0.06 cm thick, so that this time is of the order 10 milliseconds for a reasonable value of κ. Since this time is short compared to the rise time of the signal, the model of an insulated slab which is isothermal throughout is taken to represent the sample.

Writing Q for the incident radiation flux, and ρ, ℓ and C for the sample density, thickness and specific heat, respectively, the sample temperature satisfies

$$\frac{dT}{dt} = \frac{Q}{\rho \ell C} \qquad (1)$$

The variation of C with temperature is important at the low temperatures used. This variation is assumed to be adequately given by the Einstein relation:

$$C = \frac{A}{T^2} \frac{\exp (a/T)}{[\exp (a/T)-1]^2} \cong \frac{A}{T^2} \exp (-a/T) \qquad (2)$$

with the approximation which neglects the term -1, appropriate for low temperatures where a/T is large. The constants A and a are taken as adjustable parameters to give the best fit. Substituting the approximation to C into equation 1) and integrating,

$$\exp (-a/T) - \exp (-a/To) = Qat/\rho \ell A \qquad (3)$$

where To is the sample temperature at the beginning of illumination and T its subsequent temperature in degrees Kelvin.

The curves of figure 5 were made at higher temperature where the approximation of equation 2)is not justified. In these cases, however, the rise of sample temperature during illumination is reduced due to the larger specific heat at higher temperature, and the variation of

specific heat with temperature is also reduced. C is accordingly treated as a constant and equation 1) integrates directly to

$$T = \frac{Q}{\rho \ell C} t \qquad (4)$$

where T is measured in degrees Centigrade from zero at t = 0.

Equations 2) and 4) approximate the rise in sample temperature during illumination for the conditions of figures 4 and 5 . Assuming the sample to radiate as a black body, the thermal radiation reaching the detector through the 10.6 -20μ filter is given by the Planck formula as a function of the calculated temperatures. Comparison between the model and experiment is then possible using the detector calibration discussed earlier and correcting for the detector time constant. The parameters A and a are required to give a best fit to the curve of figure 4B by use of equation 3), and to the curve of figure 5B by use of equation 4) with the value of C calculated from equation 2).

Figure 6 shows the fit using a = 700°K and A = 1.25×10^6 joule gm per deg. The lines are the average signals, redrawn from figures 4B and 5B, and the circled points were calculated from the model. The degree of fit achieved is taken to indicate that the observed signals can be entirely understood in terms of increasing thermal radiation from the sample as its temperature rises during illumination.

Were prompt, luminescent radiation within the filter pass band superimposed on the thermal radiation from the sample, then the resulting rise in detector signal would appear as in figure 7. Figure 7A has been

drawn for the cases that the luminescent radiation is 5×10^{-5}, 1×10^{-4} and 5×10^{-4} watts per cm^2 from the sample surface within the 10.6 - 20μ band, and for the sample initially at -180° C. The signal calculated from the model with no luminescence is shown for comparison. It is estimated that luminescent radiation of 1×10^{-4} watts per cm^2 would have given an observable reversal of slope at the beginning of illumination of the form shown. Since the intensity of illumination was 0.4 watts per cm^2, the upper limit for luminescence efficiency at -180° C is established to be approximately 0.02 percent for the process considered in this report. Since the spectrum of the Edmund lamp is similar to that of solar radiation this upper limit applies to the case of solar illumination as well. Such a luminescent contribution is probably neglegible for lunar applications.

A luminescent contribution of this magnitude would not be detectable in this experiment for the case that the sample is at 0° C because of the greater thermal radiation. Figure 7B shows this case for several values of the intensity of prompt luminescence. The upper limit is taken as 1×10^{-3} watts per cm^2 in this case, or an upper limit for luminescence efficiency of 0.25 percent. For the case of sunlight illuminating the earth, this luminescent contribution would amount to infrared radiation between 10.6 and 20μ of some 3×10^{-4} watts per cm^2. Since thermal radiation at terrestrial temperatures exceeds this amount by two orders of magnitude such a luminescent contribution would be neglegible for terrestrial applications.

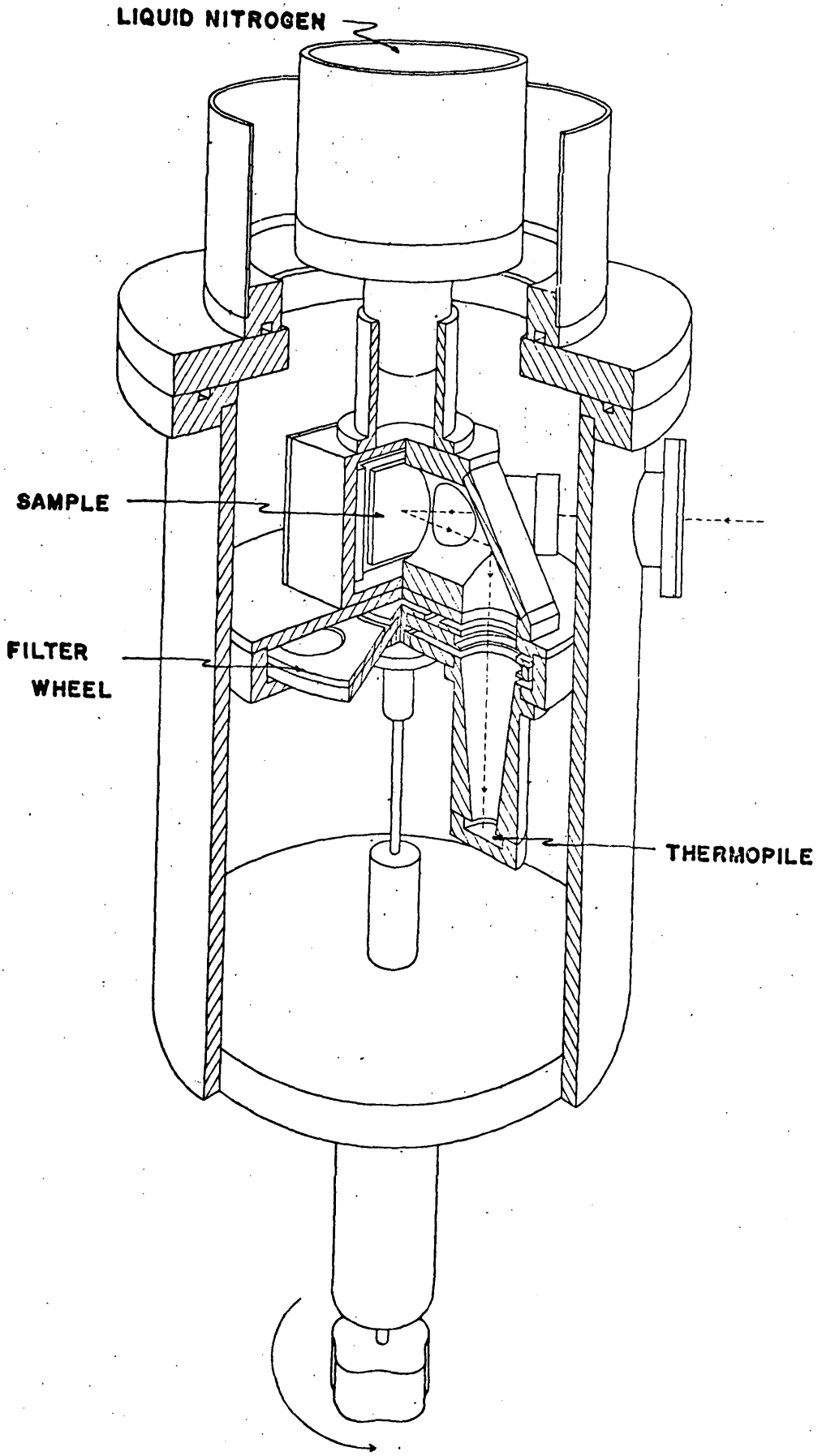

FIGURE 1
A SCHEMATIC, CUT-AWAY DRAWING OF THE DETECTOR APPARATUS

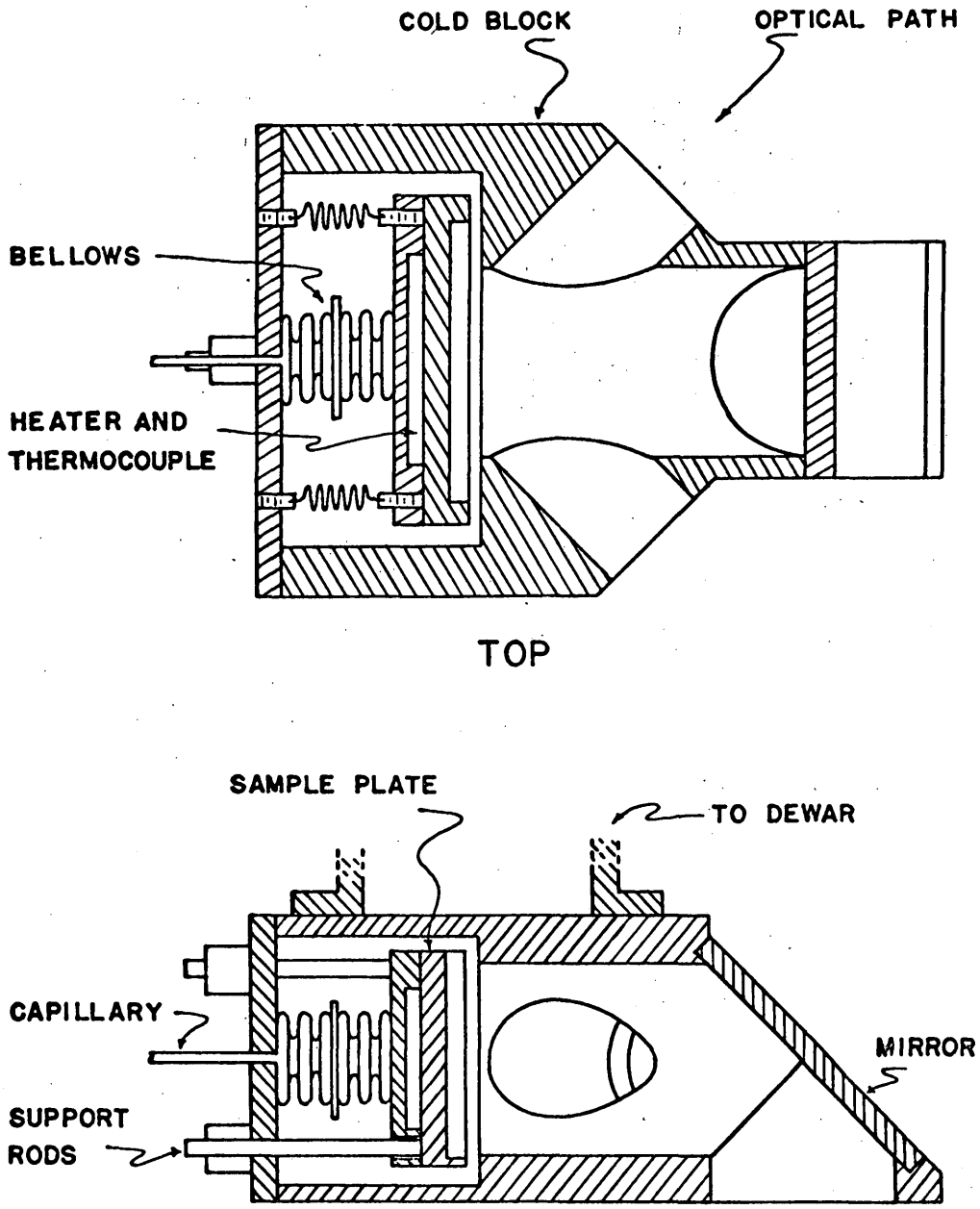

FIGURE 2

A SCHEMATIC, CUT-AWAY DRAWING OF THE SAMPLE MOUNTING

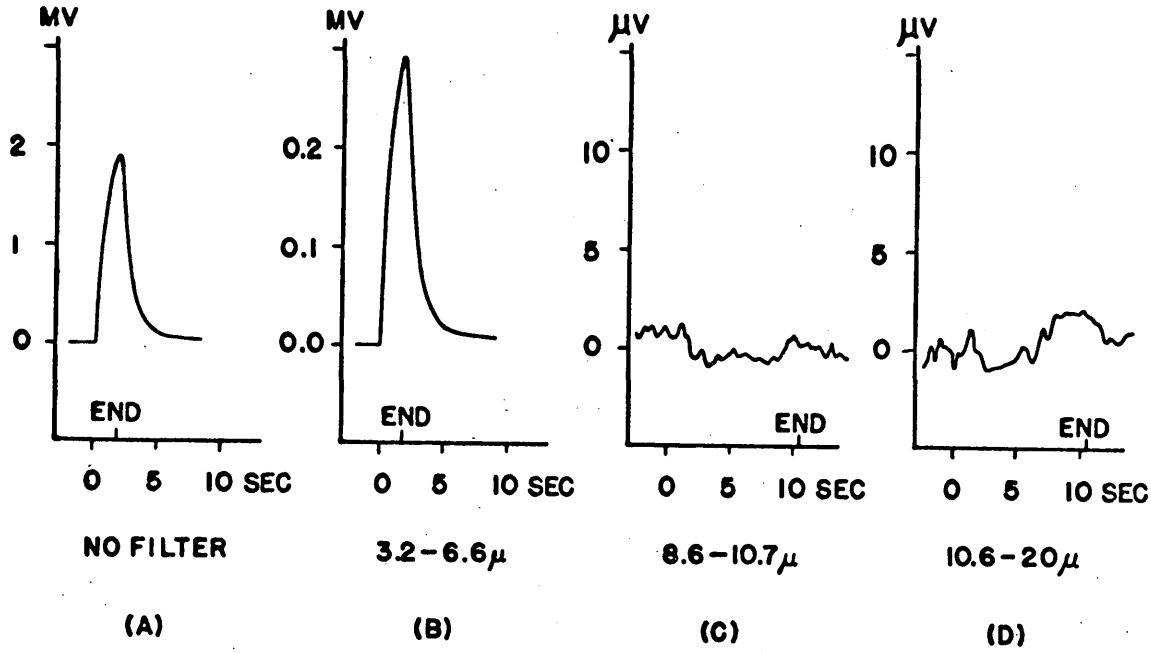

FIGURE 3

CURVES SHOWING TYPICAL RESULTS OF THE RECORDER DETECTOR SIGNAL WITH NO FILTER (A) AND AT DIFFERENT WAVELENGTHS (B), (C), (D)

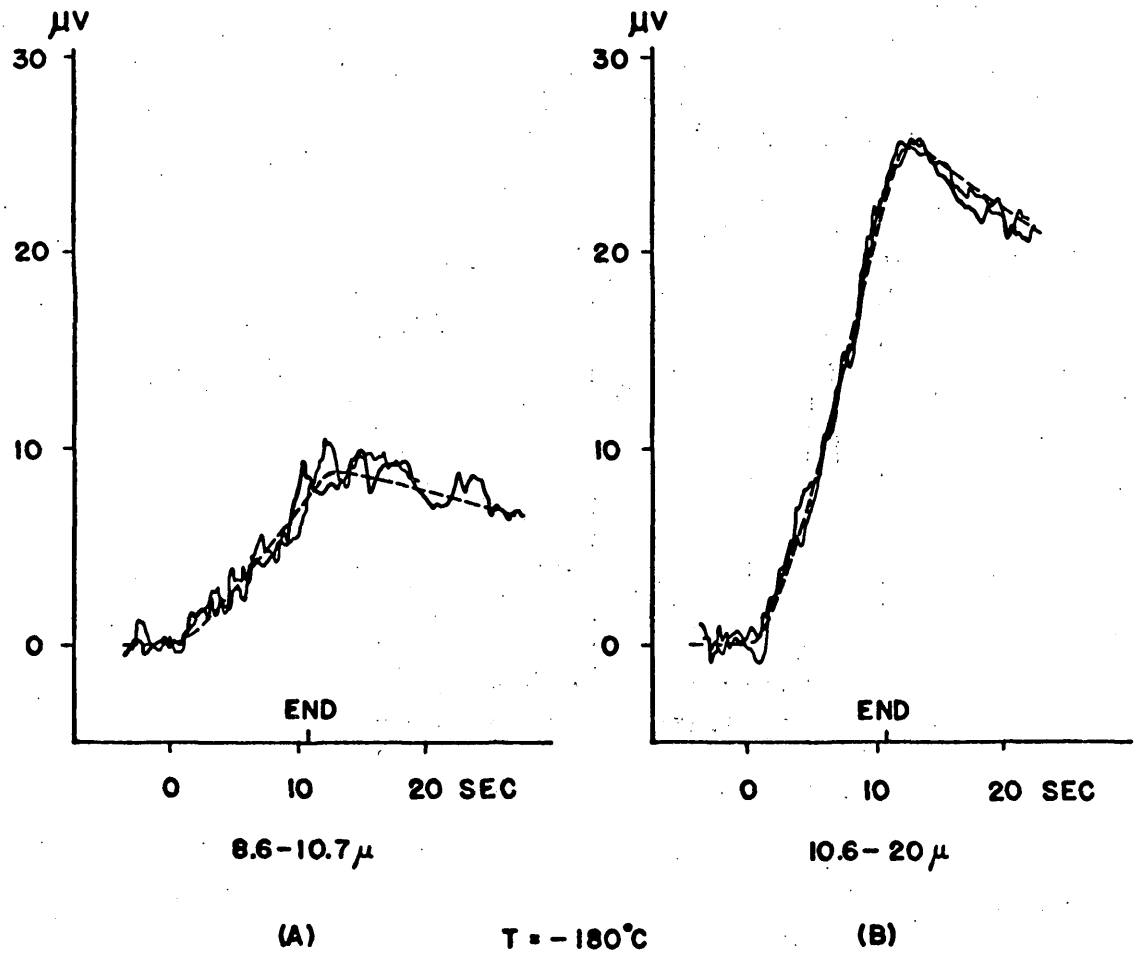

FIGURE 4

CURVES SHOWING RISE IN DETECTOR SIGNAL IN RESPONSE TO RADIATION AT DIFFERENT WAVELENGTHS WHEN T = -180°C

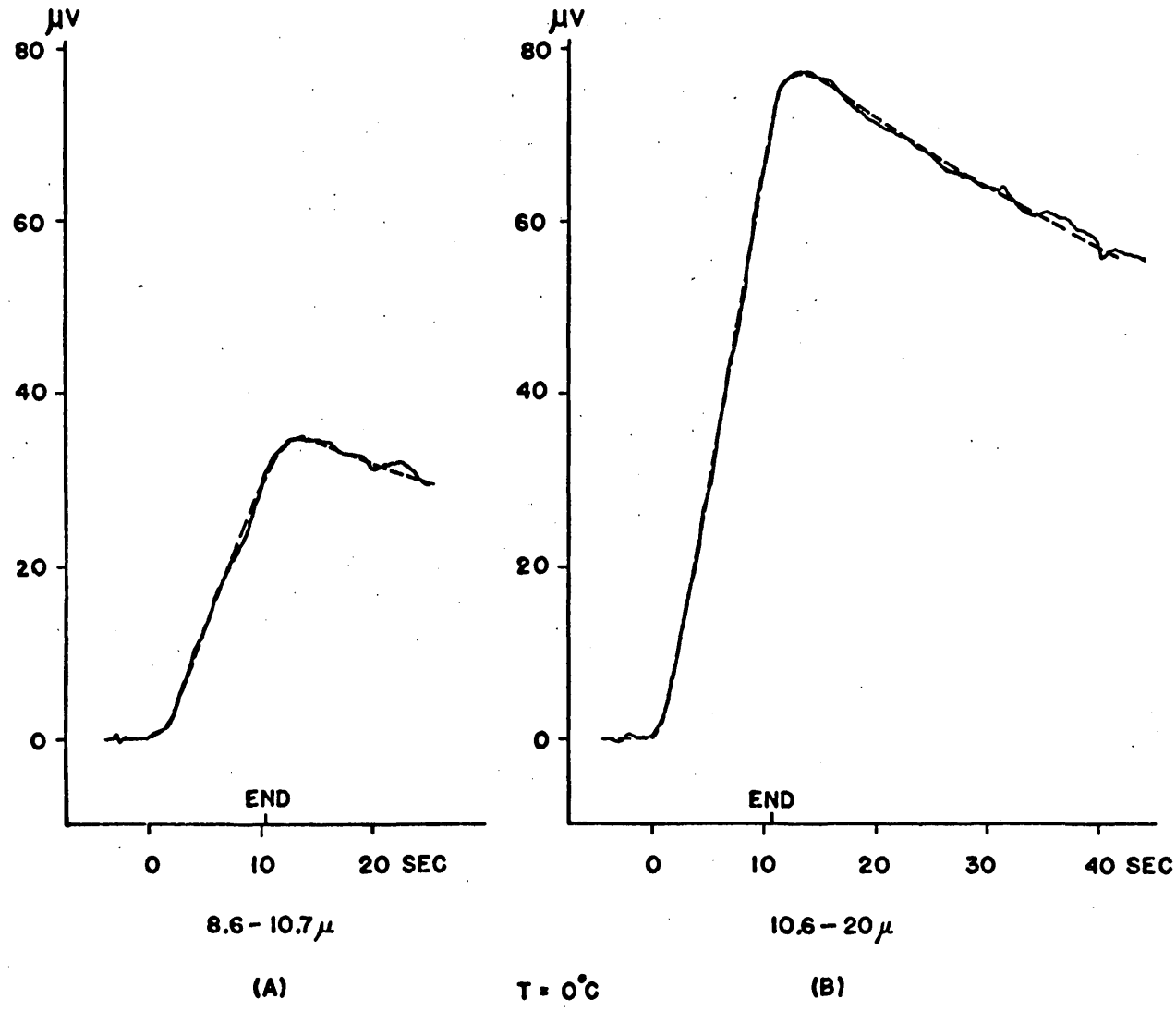

FIGURE 5

CURVES SHOWING RISE IN DETECTOR SIGNAL IN RESPONSE TO RADIATION AT DIFFERENT WAVELENGTHS WHEN T = 0°C

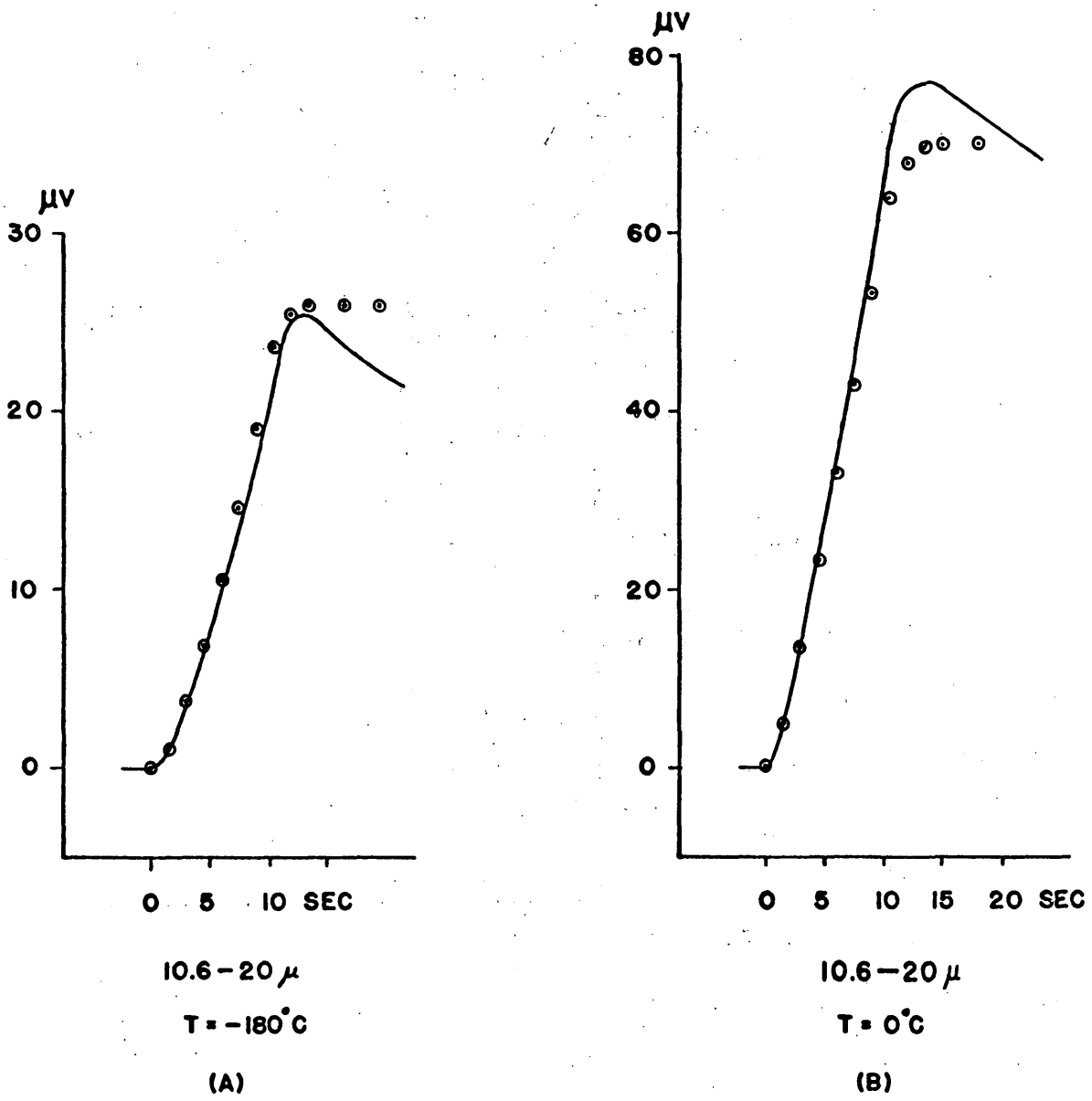

FIGURE 6

AVERAGE CURVES (LINES) SHOWING BEST FIT RELATION TO POINTS DERIVED FROM MATHEMATICAL MODEL

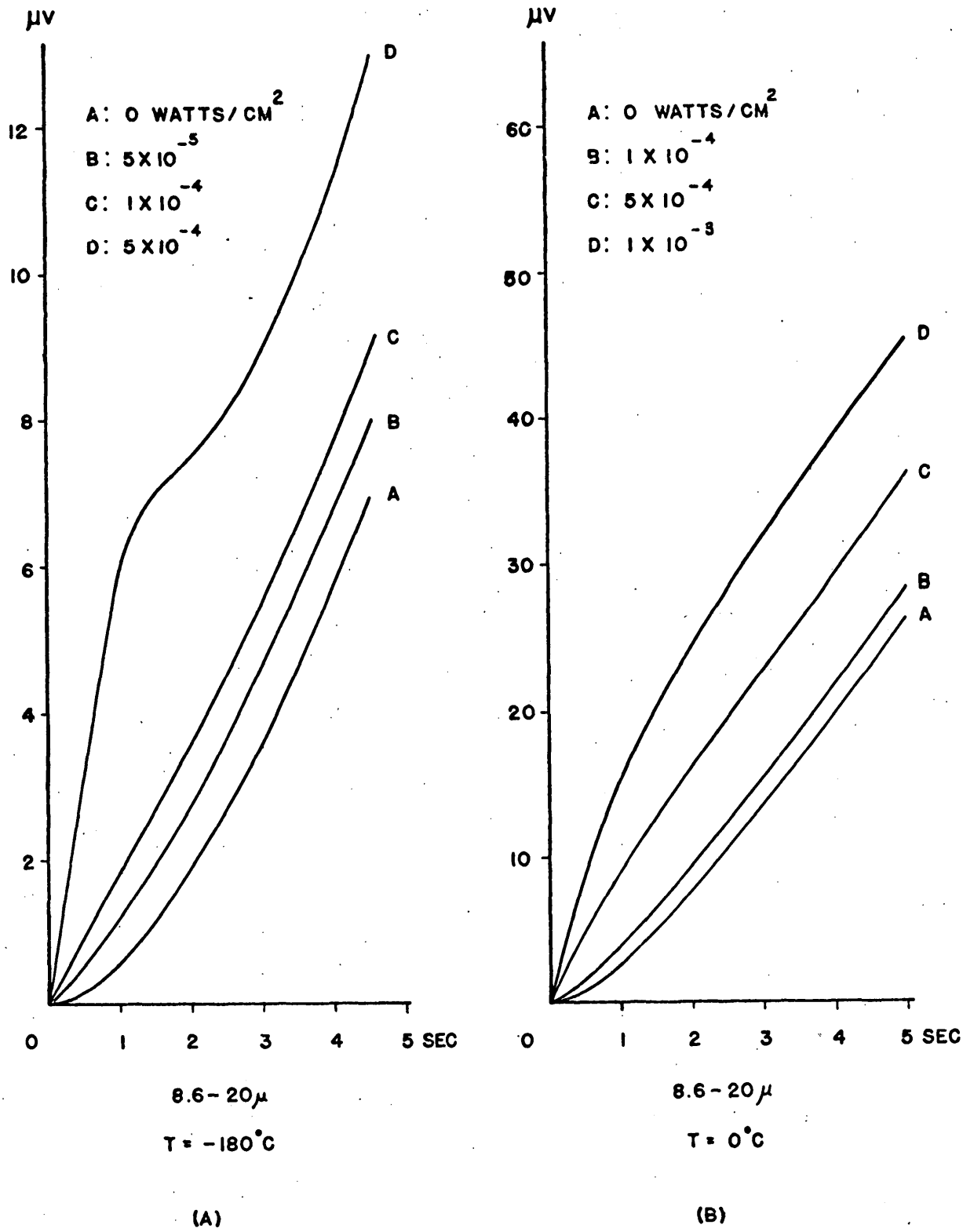

FIGURE 7
CURVES SHOWING RISE IN DETECTOR SIGNAL WHEN LUMINESCENT RADIATION WITHIN FILTER PASS BAND IS SUPERIMPOSED ON THE THERMAL RADIATION FROM THE SAMPLE, WHERE (A) T = 180°C and (B) T = 0°C